Research Square

Preprints are preliminary reports that have not undergone peer review.
They should not be considered conclusive, used to inform clinical practice,
or referenced by the media as validated information.

Explainable Deep Learning (DL) and GIS-Based Spatial Assessment of Urban River Water Quality

Md. Sojib Sheikh
International University of Business Agriculture and Technology (IUBAT)
Md. Hasan
International University of Business Agriculture and Technology (IUBAT)
Bishwajit Chandra Mazumdar
International University of Business Agriculture and Technology (IUBAT)
Mohammad Nyme Uddin
mnuddin@imamu.edu.sa
Imam Mohammad Ibn Saud Islamic University (IMSIU)

Research Article

Keywords: Water Quality Index (WQI), Deep Learning (DL), Geographic Information System (GIS), Inverse Distance Weighting (IDW), Urban River Pollution

Posted Date: November 12th, 2026

DOI: https://doi.org/10.21203/rs.3.rs-10933139/v1

License: This work is licensed under a Creative Commons Attribution 4.0 International License.
Read Full License

Additional Declarations: No competing interests reported.

Explainable Deep Learning (DL) and GIS-Based Spatial Assessment of Urban River Water Quality

Md. Sojib Sheikh[1, 2], Md. Hasan[1, 2], Bishwajit Chandra Mazumdar[1, 2], Mohammad Nyme Uddin[2, 3*]

[1] Department of Civil Engineering, College of Engineering and Technology,
International University of Business Agriculture and Technology (IUBAT), Dhaka, Bangladesh
[2] Building Energy & Environmental Management (BEEM) Enhanced by AI, Dhaka, Bangladesh
[3] Department of Architectural Engineering, College of Engineering, Imam Mohammad Ibn Saud Islamic University (IMSIU), Riyadh 11432, Saudi Arabia

21306075@iubat.edu, 21306026@iubat.edu, 21306097@iubat.edu
*Corresponding Author: mnuddin@imamu.edu.sa

Abstract

Rivers are essential freshwater resources; however, rapid urbanization, industrial discharge, and untreated municipal wastewater have significantly degraded river water quality in densely populated cities such as Dhaka, Bangladesh, threatening environmental sustainability and public health. This study aims to develop an interpretable Deep Learning (DL) and Geographic Information Systems (GIS) based framework for predicting the Water Quality Index (WQI) and identifying the dominant physicochemical and heavy metal parameters influencing water quality in the Turag, Balu, Shitalakshya, and Buriganga Rivers located in Dhaka, Bangladesh. A total of 7,616 datasets collected during the 2020-2024 monsoon season were analyzed, including eight physicochemical and eight heavy metal parameters. The Interquartile Range (IQR) method was applied for outlier detection, while normalization techniques improved data quality and predictive performance. Three DL models, namely Artificial Neural Networks (ANN), Long Short-Term Memory (LSTM), and Bidirectional Long Short-Term Memory (Bi-LSTM), were developed, and GridSearchCV was employed for hyperparameter optimization. Model performance was evaluated using Mean Squared Error (MSE), Root Mean Squared Error (RMSE), Mean Absolute Error (MAE), and the coefficient of determination (R^2). The developed ANN, LSTM, and Bi-LSTM models achieved R^2 values of 0.96, 0.99, and 0.65, respectively, with LSTM providing the best predictive performance. SHapley Additive exPlanations (SHAP) analysis identified Dissolved Oxygen (DO), turbidity, transparency, and Chemical Oxygen Demand (COD) as the most

influential variables governing WQI prediction, while GIS-based Inverse Distance Weighting (IDW) interpolation revealed significant spatial pollution hotspots across the river systems. Although the framework demonstrated strong predictive capability, the study was limited to monsoon-season observations. Future research should incorporate multi-seasonal datasets and real-time monitoring systems to improve long-term prediction and support sustainable river management.

Keywords: Water Quality Index (WQI); Deep Learning (DL); Geographic Information System (GIS); Inverse Distance Weighting (IDW); Urban River Pollution

1. Introduction

Water pollution has become one of the most pressing environmental challenges worldwide, particularly in rapidly urbanizing and industrializing regions (Mellyzar et al., 2025; Sarker et al., 2021). In developing megacities such as Dhaka, Bangladesh, uncontrolled urban expansion, population growth, industrialization, and inadequate waste management systems have contributed substantially to the deterioration of surface water quality (Yin et al., 2021). The major rivers surrounding Dhaka, including the Turag, Balu, Shitalakshya, and Buriganga Rivers, receive large volumes of industrial effluents, untreated municipal wastewater, domestic sewage, and urban runoff, resulting in severe environmental degradation (Hoque et al., 2021). Industrial sectors such as textile manufacturing, tanneries, dyeing industries, and chemical processing plants discharge wastewater containing hazardous pollutants, including heavy metals such as lead (Pb), arsenic (As), chromium (Cr), cadmium (Cd), mercury (Hg), iron (Fe), and manganese (Mn), which pose significant ecological and public health risks (Manasa & Mehta, 2020; Uddin et al., 2023). In addition, pollution alters critical physicochemical characteristics of river water, including pH, DO, biological oxygen demand (BOD), COD, electrical conductivity (EC), turbidity, total dissolved solids (TDS), total suspended solids (TSS), temperature, and transparency (Parvin et al., 2022). Consequently, the degradation of river water quality threatens aquatic ecosystems, biodiversity, and human well-being (Apandi et al., 2019; Gavrilaș et al., 2025). To simplify the interpretation of complex water quality information, the WQI is widely used as an effective tool that integrates multiple physicochemical and heavy metal parameters into a single numerical value representing overall water quality conditions (Iwar et al., 2021). Therefore, accurate assessment and prediction

of WQI are essential for pollution monitoring, environmental planning, and sustainable urban river management.

Traditionally, water quality assessment has relied on periodic field sampling and laboratory-based analyses to evaluate the status of aquatic environments (Paepae et al., 2021). Although these approaches provide reliable measurements, they are often labor-intensive, time-consuming, and costly, making continuous monitoring difficult in highly dynamic urban river systems. Furthermore, conventional monitoring programs frequently struggle to process large volumes of environmental data and rapidly changing pollution conditions, resulting in delayed detection of water quality deterioration (Ahmed et al., 2020). To analyze relationships among water quality variables, researchers have widely employed statistical techniques such as correlation analysis, regression models, and trend analysis (van den Broeke et al., 2013). While these approaches provide valuable insights into pollutant dynamics, they are often limited in their ability to capture the nonlinear, complex, and time-dependent interactions that characterize urban river ecosystems. As a result, more advanced analytical approaches are needed to improve the accuracy and reliability of water quality prediction.

Recent advances in DL have created new opportunities for environmental monitoring and water quality assessment. DL models can effectively process large environmental datasets and capture complex nonlinear relationships among water quality variables (Ahmed et al., 2023). Among these approaches, ANN, LSTM, and Bi-LSTM models have demonstrated promising performance in water quality prediction studies. ANN models are effective in modeling nonlinear environmental relationships, whereas LSTM and Bi-LSTM architectures are particularly suitable for learning temporal dependencies and sequential patterns in environmental data (Khosravi et al., 2025; Sekarlangit et al., 2024). In addition to predictive modeling, unsupervised learning techniques such as Density-Based Spatial Clustering of Applications with Noise (DBSCAN) and hierarchical clustering provide valuable tools for identifying hidden pollution patterns, grouping similar water quality conditions, and detecting anomalous observations within complex environmental datasets (Kazemi & Soleimani, 2025). Furthermore, GIS offers powerful capabilities for spatial visualization, pollution hotspot identification, and assessment of geographic variations in water quality. Despite these advances, previous studies have often focused on conventional statistical approaches or individual Machine Learning (ML) models, with limited efforts to integrate

clustering techniques, DL, and GIS within a unified framework for comprehensive urban river water quality assessment. Moreover, the interpretability of DL predictions remains a challenge, highlighting the need for explainable approaches capable of identifying the key factors driving water quality changes.

This study develops an integrated framework combining clustering analysis, DL, and GIS-based spatial assessment to predict the WQI and identify the dominant factors influencing river water quality in the Turag, Balu, Shitalakshya, and Buriganga Rivers surrounding Dhaka, Bangladesh. Specifically, the study applies data preprocessing and outlier detection techniques to improve data quality, employs anomaly detection to explore pollution patterns and spatial-temporal similarities within water quality observations, develops and compares ANN, LSTM, and Bi-LSTM models for WQI prediction, and utilizes SHAP to interpret model outputs and determine the most influential physicochemical and heavy metal parameters affecting water quality. Furthermore, GIS-based spatial interpolation is used to identify pollution hotspots and examine spatial variations across the river systems. The proposed framework is expected to provide reliable WQI prediction, enhanced understanding of pollution dynamics, and valuable decision-support information for sustainable urban river management and environmental protection.

The remainder of this paper is organized as follows. Section 2 reviews the literature on WQI prediction, DL, and GIS-based water quality assessment. Section 3 describes the study area, dataset, and research methodology. Section 4 presents the results of the developed models and spatial analyses. Section 5 discusses the key findings and their implications. Finally, Section 6 concludes the study and outlines future research directions.

2. Literature Review

2.1 Existing Approaches for WQI Monitoring and Prediction

Several studies have demonstrated the effectiveness of DL based approaches for water quality prediction. Study by (Sharmaa & Panditb) applied regression and correlation analysis to evaluate relationships among physicochemical parameters and pollution indicators in river systems. Another study (Ma & Chen, 2025) used Auto Regressive Integrated Moving Average (ARIMA)

based time-series analysis for forecasting river pollution trends using historical water quality data. Recent research has also employed ANN, Random Forest (RF), Extreme Gradient Boosting (XGBoost), and Convolutional Neural Network (CNN)-LSTM frameworks for WQI prediction, where ANN and RF achieved strong predictive performance in urban river environments (Nishat et al., 2025). Similarly study by (Karbasi et al., 2024) integrated Boruta Feature Selection Algorithm (Boruta)-XGB-CNN-LSTM models for EC forecasting and demonstrated improved prediction accuracy using sequential learning techniques. Furthermore, explainable AI approaches such as SHAP have increasingly been used to identify dominant environmental drivers influencing water quality prediction and improve model interpretability (Zhang et al., 2025). However, many studies remain limited by insufficient spatial coverage, dependence on historical observations, and a lack of integration between DL and GIS-based spatial assessment. **Table 1** summarizes the techniques used for water quality prediction and evaluation across different regions, including ML models.

132 Table 1: Summary of Techniques Used in Water Quality Prediction and Evaluation

Year of Study	Country / Location	Tasks	Methods	Sample Type	Input Parameters	Findings	Limitations	References
2017–2018	Uttar Pradesh, India (River Chhoiya)	Assess river water quality and predict physicochemical parameters	Correlation and linear regression analysis across seasons and stations	River water samples	pH, EC, TDS, alkalinity, hardness, TSS, nitrate, sulphate, DO, BOD, COD, turbidity	Significant linear relationships among parameters were identified. Stations B and C exceeded permissible limits, indicating severe pollution and industrial discharge impacts.	Limited to conventional regression analysis without AI/DL models, GIS mapping, SHAP interpretation, clustering, heavy metal analysis, or nonlinear temporal prediction used in the present study.	(Sharmaa & Panditb)
2019–2023	Yangtze River, China	Predict total phosphorus (TP) variation and monitor water quality	Time series analysis, data mining, and MTS-Mixers prediction model	River water quality time-series data	Total phosphorus (TP)	The optimized MTS-Mixers model achieved high prediction accuracy and effectively captured TP temporal variations.	Focused only on TP prediction without integrated WQI assessment, GIS spatial analysis, SHAP explainability, clustering methods, or multi-parameter deep learning frameworks used in the present study.	(Ma & Chen, 2025)
2001–2023	Dhaka, Bangladesh (Buriganga, Balu, Tongi Khal, Turag)	Predict WQI and compare ML models for urban river monitoring	14 ML models including ANN, RF, XGB, SVM, GBM, CatBoost	River water quality dataset (262 samples)	DO, pH, EC, TDS, Fe, Cl	ANN and RF showed best performance with high WQI prediction accuracy (R^2 = 0.97).	Limited physicochemical parameters and small sample size. Did not integrate LSTM/Bi-LSTM, SHAP, GIS-IDW, clustering, or extensive heavy metal analysis as used in the present study.	(Nishat et al., 2025)
2012–2021	Australia (Albert River and Barratta Creek)	Forecast EC up to 10 days ahead	Boruta-XGB feature selection with CNN-LSTM, compared with MLP, KNN, XGBoost	River water time-series data	EC lagged time-series data	Boruta-XGB-CNN-LSTM showed superior EC forecasting performance up to 10 days ahead.	Focused only on EC forecasting without WQI prediction, GIS mapping, SHAP analysis, clustering, or multi-parameter environmental assessment used in the present study.	(Karbasi et al., 2024)
2019	Xinjiang Province, China (Manas River Basin)	Evaluate groundwater quality and identify pollution indicators	XGBoost, SHAP analysis, PMF	Groundwater samples (187 sites)	Zn, nitrate, chloride, Mn, pH, conductivity, turbidity	Zinc, nitrate, and chloride were identified as dominant pollution indicators through interpretable AI analysis.	Focused on groundwater rather than urban river WQI prediction. Did not include GIS-IDW, clustering, temporal deep learning, or comparative ANN/LSTM/Bi-LSTM analysis.	(Zhang et al., 2025)
2015	United States	Predict Total Suspended Solids (TSS) concentration	LR, kNN, SVR, ANN, RT, RF, AdaBoost	Stormwater quality database	Drainage area, land use, imperviousness, rainfall depth, runoff volume	AdaBoost and RF achieved the best TSS prediction performance.	Focused only on TSS prediction without WQI assessment, GIS mapping, SHAP, clustering, temporal deep learning, or heavy metal analysis. Dataset also contained missing values.	(Moeini et al., 2021)
2000–2021	Pearl River Estuary, China	Estimate spatial-temporal variation of TSS and Chl-a	XGBoost and BPNN	Estuarine and coastal water data	TSS and Chlorophyll-a	XGBoost outperformed BPNN and identified strong seasonal and spatial variation patterns.	Focused mainly on TSS and Chl-a without WQI prediction, SHAP explainability, clustering, or deep learning integration used in the present study.	(Liu et al., 2023)
2023	Mexico (Lake Chapala)	Predict TSS using remote sensing and AI	Multiple regression with unsupervised ML and Landsat imagery	Lake monitoring and satellite data	Remote sensing spectral data and TSS	The model achieved good TSS prediction accuracy using remote sensing approaches.	Focused only on TSS estimation without WQI prediction, SHAP analysis, clustering, heavy metal assessment, or LSTM/Bi-LSTM models.	(Torres-Vera, 2023)

2020	Bangladesh (Turag River)	Assess heavy metals and PAHs in sediments	Geo-accumulation index, enrichment factor, PCA, correlation analysis	Sediment samples from 11 stations	26 elements and PAHs	Zn was identified as the major contaminant, with strong anthropogenic pollution influence.	Focused on sediment contamination rather than WQI prediction. Did not apply AI/DL models, SHAP, GIS-IDW, clustering-based prediction, or temporal forecasting.	(Khan et al., 2020)
2025	Global urban water systems	Review AI-driven predictive water quality monitoring	Review of AI, IoT, ML, DL, and hybrid models	IoT sensor and monitoring datasets	pH, turbidity, DO, conductivity	AI and IoT integration improved real-time monitoring and contamination forecasting.	Review-based study without experimental validation, GIS-IDW mapping, SHAP, clustering, or ANN/LSTM/Bi-LSTM implementation.	(Ahamad & Singh, 2025)
2025	Bangladesh (Turag River)	Assess pollution sources and river water quality	GIS spatial analysis and WQI assessment	River water samples from 9 sites	pH, DO, BOD, TSS, turbidity, phosphate, nitrate, temperature	WQI classified all sampling locations as "Bad," indicating severe industrial pollution.	Limited parameters and sampling coverage. Did not apply AI/deep learning models, SHAP, clustering, heavy metal analysis, or ANN/LSTM/Bi-LSTM frameworks used in the present study.	(Rony et al., 2025)
Present Study (2020-2024)	Dhaka, Bangladesh (Turag, Balu, Shitalakshya, Buriganga Rivers)	Predict WQI, identify dominant pollution indicators, and assess spatial pollution variability	ANN, LSTM, Bi-LSTM, SHAP analysis,	River water samples (7,616 observations)	pH, DO, turbidity, transparency, EC, COD, BOD, TDS, Cd, Cr, Ni, Pb, and other heavy metals	LSTM achieved the best prediction performance (R^2 = 0.99). SHAP identified DO, turbidity, transparency, and COD as dominant WQI drivers. GIS-IDW mapping revealed major pollution hotspots across the river systems.	The study was limited to monsoon-season observations and depended on available monitoring datasets. Future studies should incorporate multi-seasonal monitoring, real-time sensor systems, satellite data, and hybrid AI frameworks for improved long-term prediction and management.	Present study

133

2.2 DL and GIS-Based Approaches

Recent studies have increasingly adopted DL and GIS-based techniques to overcome the limitations of traditional water quality assessment methods. Study by (Moeini et al., 2021) applied RF, Adaptive Boosting (AdaBoost), k-Nearest Neighbors (kNN), Support Vector Regression (SVR), and ANN models for environmental prediction, where ensemble and ANN-based models showed strong capability despite some overfitting issues. Another study (Liu et al., 2023) applied XGBoost and Backpropagation Neural Networks (BPNN) to analyze spatial and temporal water quality characteristics, although performance was constrained by limited datasets.

Further advancements include the integration of remote sensing, explainable DL and GIS-based spatial analysis. Study by (Torres-Vera, 2023) used Landsat spectral bands and ML techniques for large-scale water quality monitoring through satellite imagery. In addition, explainable DL approaches such as SHAP are increasingly used to identify dominant environmental variables influencing prediction outcomes and improve model interpretability. GIS-based interpolation techniques such as IDW are also widely applied to visualize pollution distribution and identify hotspot regions in river systems. IDW-based spatial mapping enables continuous visualization of physicochemical parameters, heavy metals, and pollution intensity from discrete sampling locations, supporting pollution hotspot detection and environmental management in urban river environments.

2.3 Studies on the Turag, Balu, Shitalakshya, and Buriganga Rivers

Several studies have investigated pollution and water quality degradation in the major urban rivers surrounding Dhaka, including the Turag, Balu, Shitalakshya, and Buriganga Rivers. (Khan et al., 2020) analyzed heavy metals and polycyclic aromatic hydrocarbons (PAHs) in Turag River sediments, identifying Zn as the dominant contaminant and indicating strong anthropogenic influence from industrial and urban activities. The study also reported potential ecological risks associated with sediment contamination and emphasized the need for more integrated investigations involving water quality and pollutant interactions.

Another study (Islam et al., 2023) assessed seasonal variations of physicochemical parameters in the Buriganga and Turag Rivers and reported elevated levels of turbidity, BOD, COD, and EC during the dry season due to reduced dilution capacity and increased industrial discharge. The

study highlighted severe organic and chemical pollution in densely urbanized river sections but was limited by short-term monitoring duration. Another study (Rony et al., 2025) evaluated water quality conditions in rivers surrounding Dhaka using GIS and WQI analysis, revealing severe pollution caused by untreated industrial discharge, municipal wastewater, and urban runoff. Elevated turbidity, BOD, COD, and EC values were observed across multiple sampling locations in the Turag, Buriganga, Balu, and Shitalakshya Rivers, indicating significant spatial variability in pollution intensity. However, the study was limited by restricted physicochemical parameters and limited temporal monitoring.

Similarly study by (Suchi et al., 2024) assessed physicochemical characteristics and heavy metal contamination in the river systems around Dhaka and identified ecological and human health risks associated with heavy metals such as Hg, Cd, and As. The findings indicated that industrial effluents, urban runoff, and anthropogenic activities were the primary contributors to river pollution. Nevertheless, the study was constrained by limited spatial and seasonal sampling coverage, highlighting the need for more comprehensive predictive and spatial assessment frameworks for these urban river systems. Furthermore, a comprehensive baseline evaluation conducted by (Nishat et al., 2025) compared fourteen different machine learning architectures to forecast the WQI across the Buriganga, Balu, Turag, and Tongi Khal waterways. Their work highlighted that while traditional regression models struggle with complex river datasets, ANN and RF algorithms achieve optimal predictive capabilities. However, this study noted that predictive accuracy is heavily contingent on handling data inconsistencies across diverse urban environments.

2.4 Research Gap and Contribution of This Study

Despite recent advancements in water quality prediction assessment, studies integrating DL preprocessing techniques and GIS-based spatial assessment remain limited, particularly for urban rivers in developing countries such as Bangladesh. Most previous studies primarily focused on conventional monitoring, standalone ML models, or spatial analysis independently, without developing a comprehensive framework that simultaneously addresses prediction accuracy, feature importance interpretation, temporal dependency learning, and spatial pollution variability across multiple river systems.

To address these limitations, the present study develops an integrated DL and GIS framework for WQI prediction and spatial assessment in the Turag, Balu, Shitalakshya, and Buriganga Rivers, Bangladesh. The study employs ANN, LSTM, and Bi-LSTM models combined with SHAP-based interpretation and GIS-IDW spatial mapping to identify dominant environmental drivers and visualize pollution hotspot distributions across the river systems. Additionally, IQR-based outlier detection and normalization techniques are applied to improve data quality and predictive model performance. The proposed framework contributes to accurate, interpretable, and spatially explicit water quality assessment for sustainable river management in highly urbanized and industrialized regions.

3. Methodology

This study adopted a systematic and integrated methodology to assess river water quality in the Turag, Balu, Shitalakshya, and Buriganga Rivers surrounding Dhaka city. The proposed framework comprised five interrelated stages: data collection, data preprocessing, clustering-based exploratory analysis, DL-based predictive modeling, and GIS-based spatial assessment and pollution hotspot mapping, illustrated in the methodological flowchart (**Figure 1**).

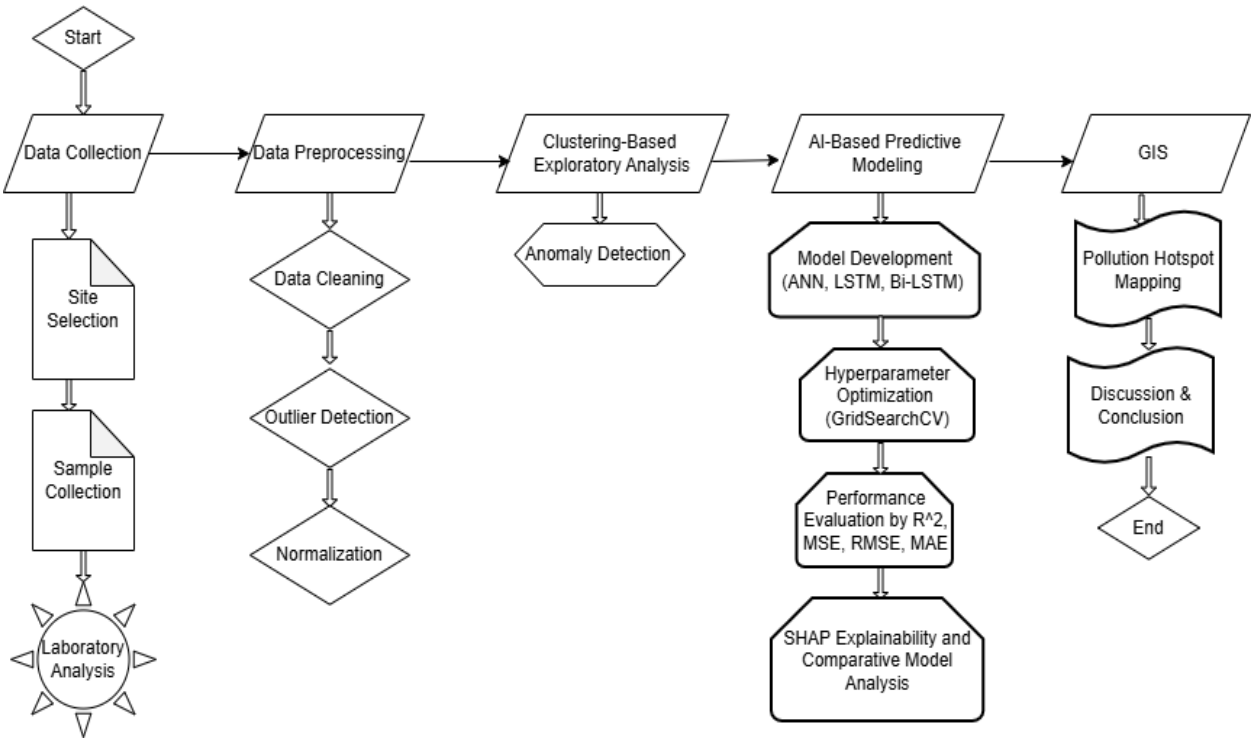


Figure 1. Methodological Framework

3.1 Site Selection

The study was conducted in the four major rivers surrounding Dhaka city, Bangladesh, including the Turag, Balu, Shitalakshya, and Buriganga rivers (**Figure 2**). These rivers are important urban water bodies supporting domestic, agricultural, industrial, and economic activities in a densely populated metropolitan region. They also sustain aquatic ecosystems and help maintain environmental balance. However, rapid urbanization, industrialization, and untreated wastewater discharge have severely degraded water quality, raising serious environmental and public health concerns. The study area has a subtropical monsoon climate with distinct wet and dry seasons that strongly influence river flow and water quality dynamics (Miah et al., 2025). Due to their high pollution levels and ecological importance, these river systems have become major environmental concerns in Dhaka, highlighting the need for comprehensive water quality assessment and effective pollution management strategies.

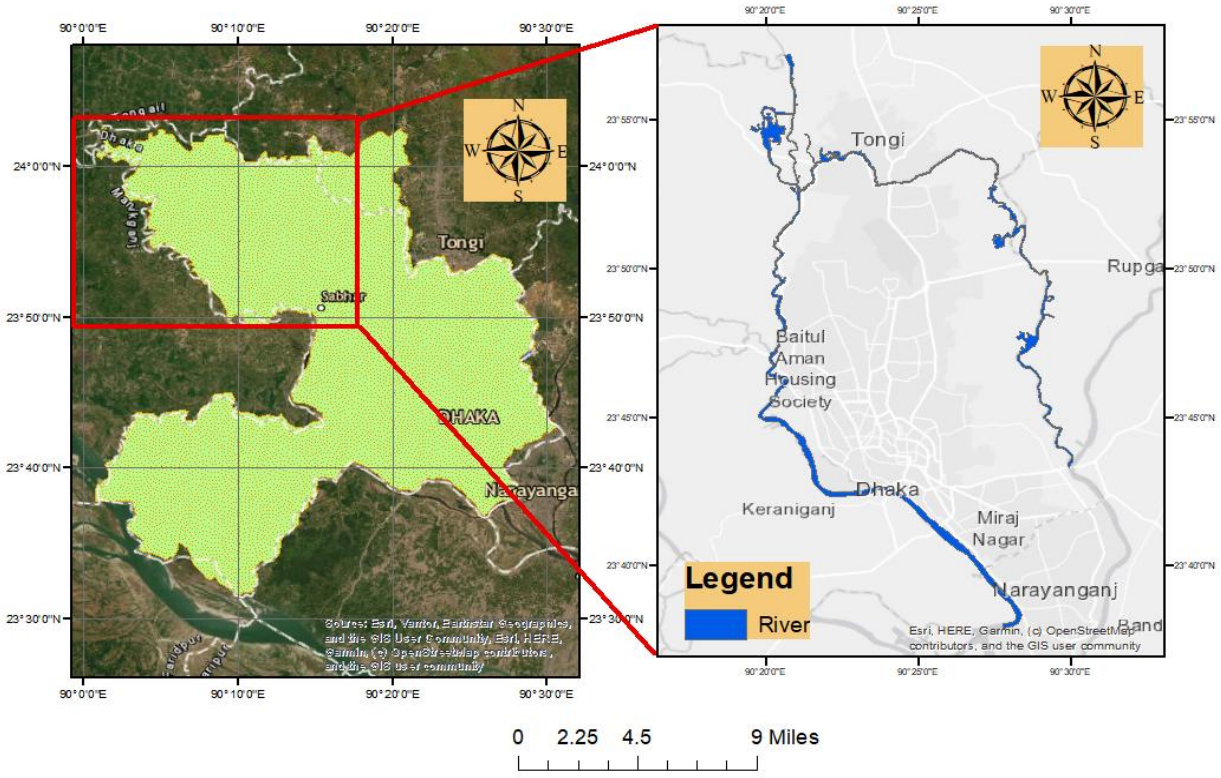


Figure 2. Sampling points along the multiple rivers

3.2 Sample Collection

A total of 7,616 observations were collected from multiple monitoring stations through repeated seasonal sampling during the monsoon periods (June to October) from 2020 to 2024 across the Turag, Balu, Shitalakshya, and Buriganga rivers. The collected samples were analyzed to assess variations in physicochemical parameters, heavy metal concentrations, and overall pollution conditions within the study area. Heavy metals measured included Ni, Mn, Fe, Cu, Cr, Cd, Zn, and Pb, while physicochemical parameters included pH, DO, EC, COD, turbidity, transparency, temperature, and TDS. These parameters were used to evaluate key aspects of water quality, including acidity, oxygen availability, ionic concentration, organic pollution load, water clarity, thermal conditions, and overall dissolved substance content in the aquatic environment.

3.3 Sampling Process and Laboratory Test

Water samples were collected from multiple monitoring locations during the monsoon periods (June to October) from 2020 to 2024 to assess spatial and temporal variations in physicochemical characteristics and heavy metal contamination associated with industrial discharge, municipal wastewater, and urban runoff. Grab sampling techniques were employed at selected monitoring sites using pre-cleaned polyethylene bottles thoroughly rinsed with distilled water to minimize contamination risks. Immediately after collection, all samples were sealed, labeled, and preserved following APHA Standard Methods to ensure data reliability for laboratory analysis (Association et al., 1905). A detailed list of analytical instruments is provided in **Table 2**. Geographic coordinates of all sampling locations were recorded to support GIS-based spatial analysis and pollution hotspot mapping. This approach enabled a comprehensive assessment of river water quality dynamics under varying hydrological and climatic conditions.

Table 2. Laboratory-based Chemical Parameters and Methods

Parameter	Description	Unit	Instrument/Method Used
pH	Indicates acidity or alkalinity of water	–	Portable pH Meter
DO	Measures dissolved oxygen available for aquatic life	mg/L	Winkler Titration Method / DO Meter
EC	Indicates ionic concentration and conductivity of water	µS/cm	Electrical Conductivity Meter
COD	Measures total oxidizable pollutants in water	mg/L	COD Reactor and Photometer

Turbidity	Represents optical clarity and suspended particles	NTU	Portable Turbidity Meter
Transparency	Indicates water clarity and light penetration	in	Secchi Disk Method
Temperature	Measures thermal condition of water	°C	Digital Thermometer
TDS	Indicates total dissolved substances in water	mg/L	TDS Meter
Ni	Measures the nickel contamination level	mg/L	Atomic Absorption Spectrophotometer (AAS)
Mn	Measures manganese concentration	mg/L	Atomic Absorption Spectrophotometer (AAS)
Fe	Measures iron concentration	mg/L	Atomic Absorption Spectrophotometer (AAS)
Cu	Measures copper contamination level	mg/L	Atomic Absorption Spectrophotometer (AAS)
Cr	Measures chromium contamination level	mg/L	Atomic Absorption Spectrophotometer (AAS)
Cd	Measures cadmium concentration	mg/L	Atomic Absorption Spectrophotometer (AAS)
Zn	Measures zinc concentration	mg/L	Atomic Absorption Spectrophotometer (AAS)
Pb	Measures lead contamination level	mg/L	Atomic Absorption Spectrophotometer (AAS)

3.4 Data Preprocessing:

The collected water quality dataset was subjected to a systematic preprocessing procedure to ensure data quality and reliability prior to clustering and DL-based predictive modeling. The preprocessing stage consisted of three sequential steps: data cleaning, outlier detection, and normalization, as illustrated in **Figure 1**. Initially, data cleaning was performed to remove incomplete, duplicate, and inconsistent records, thereby improving dataset consistency and reducing potential bias in subsequent analyses. Following this, outlier detection was conducted using the IQR method to identify abnormal observations in both physicochemical and heavy metal parameters (Wan et al., 2014). Given the non-normal distribution and strong seasonal variability of river water quality data, the IQR method was adopted because of its robustness in handling skewed environmental datasets. The interquartile range was defined as the difference between the third quartile (Q3) and the first quartile (Q1), as shown in **Equation 1**.

$IQR = Q_3 - Q_1$ ……..(1)

Observations falling outside the lower and upper bounds were classified as outliers according to **Equation 2**.

$X < Q_1 - 1.5(IQR)$ or $x > Q_3 + 1.5(IQR)$ ……(2)

where X represents an individual observation. Identified outliers were carefully evaluated and removed to reduce noise while preserving meaningful environmental variability.

Finally, normalization was applied to standardize parameter scales, improving compatibility across variables and enhancing the performance of clustering and predictive models. The effectiveness of preprocessing was assessed through boxplot comparisons before and after demonstrating improved distribution consistency and reduced influence of extreme values across water quality parameters.

3.5 WQI

The WQI was used to assess the overall river water quality and provide an integrated representation of pollution status within the study area. It is widely applied to simplify complex water quality datasets into a single numerical value for easier interpretation and environmental management. In this study, the weighted arithmetic index method was adopted for WQI computation due to its suitability for environmental water quality assessment (Subramanian & Baskar, 2022). Standard permissible limits for each parameter were obtained from the World Health Organization (WHO) drinking water guidelines and the Bangladesh Department of Environment (DoE) standards, where applicable. The WQI calculation involved several sequential steps. First, the proportionality constant (K) was computed based on the standard permissible values (Sn) of all parameters, as shown in **Equation 3**.

$$K = \frac{1}{\sum(\frac{1}{Sn})} \quad \text{……(3)}$$

Next, the quality rating for each parameter (Qn) was determined using **Equation 4**.

$$Qn = \left(\frac{Vn - Vio}{Sn - Vio}\right) \times 100 \quad \text{……..(4)}$$

where Qn represents the quality rating of the nth parameter, V_n is the observed value, and Vio is the ideal value under natural conditions.

The unit weight (W_n) for each parameter was then calculated using **Equation 5**.

$$Wn = \frac{K}{Sn} \quad \text{.....(5)}$$

Finally, the overall WQI was obtained through weighted aggregation, as expressed in **Equation 6**.

$$WQI = \frac{\sum(WnQn)}{\sum Wn} \quad \text{.....(6)}$$

3.6 Clustering-Based Exploratory Analysis

Clustering-based exploratory analysis was conducted to identify hidden pollution patterns and similarity structures within the water quality dataset. Unsupervised ML techniques, were applied to group observations based on physicochemical and heavy metal characteristics. Anomaly detection was utilized to detect dense pollution clusters and identify anomalous observations, while Hierarchical Clustering was used to examine similarity relationships among sampling locations. Prior to clustering, the dataset was preprocessed through data cleaning, outlier removal, and normalization to ensure scale consistency and improve clustering performance (Odong et al., 2013). The resulting cluster structures were used to characterize pollution zones and spatial patterns, which were subsequently integrated with deep learning-based predictive modeling and GIS-based spatial visualization for comprehensive water quality assessment.

3.7 DL-Based Prediction Model

The development and training of DL models to predict the WQI using physicochemical and heavy metal parameters. Three deep learning architectures, including ANN, LSTM, and Bi-LSTM, were implemented to evaluate nonlinear and sequential learning capabilities for river water quality prediction. These models were selected due to the complex, nonlinear, and highly dynamic nature of river water quality data, which is influenced by industrial discharge, seasonal hydrological variation, and mixed pollutant sources. Traditional statistical models often fail to capture such nonlinear interactions effectively, whereas deep learning approaches are capable of learning complex feature representations from high-dimensional environmental datasets. In particular, ANN is suitable for modeling nonlinear relationships, while LSTM and Bi-LSTM are effective in

capturing temporal dependencies and sequential variability in water quality parameters. The ANN model served as a baseline predictive approach using multiple dense hidden layers. The LSTM model was designed to learn sequential dependencies through gated memory structures, where the hidden state update mechanism is defined in **Equation 7**.

$$h_t = \emptyset(W_x x_t + W_h h_{t-1} + b) \quad \text{.....(7)}$$

where h_t denotes the hidden state at time t, x_t is the input vector, W_x and W_h are weight matrices, and b is the bias term. The Bi-LSTM architecture extends this framework by processing information in both forward and backward directions, improving feature learning and predictive accuracy.

The dataset was divided into training (80%) and testing (20%) subsets. Hyperparameter optimization was performed using GridSearchCV to identify optimal configurations, including learning rate, batch size, hidden units, dropout rate, and epochs. To improve generalization performance, dropout regularization and early stopping were applied during training. All models used ReLU activation functions in hidden layers and a linear activation function in the output layer for continuous WQI prediction. The models were implemented in Python using TensorFlow, Keras, Scikit-learn, NumPy, and Pandas, with GPU acceleration to improve computational efficiency. The Adam optimizer with a learning rate of 0.001 was used to ensure stable convergence during training. An overview of the ANN, LSTM, and Bi-LSTM architectures, including layer configurations and parameter sizes, is provided in **Appendix 1.** All models were trained using the MSE loss function, defined in **Equation 8**.

$$MSE = \frac{1}{m}\sum_{i=1}^{m}(y_i - \hat{y}_i)^2 \quad \text{..... (8)}$$

The parameter update rule of the Adam optimizer is expressed in **Equation 9**.

$$\theta_t = \theta_{t-1} - \frac{m_t}{\sqrt{v_t} + \epsilon} \quad \text{.....(9)}$$

where θ_t is the updated parameter vector, m_t is the first moment estimate, v_t is the second moment estimate, and ε is a small constant for numerical stability. Model performance was evaluated using MAE, RMSE, and R^2. These metrics are defined in **Equations 10 - 12**.

$$MAE=\frac{1}{n}\sum_{i=1}^{n}|yi-\hat{y}i| \quad \text{.....(10)}$$

$$RMSE=\sqrt{\frac{1}{m}\sum_{i=1}^{m}(yi-\hat{y}i)^2} \quad \text{.....(11)}$$

$$R^2=1-\frac{\sum_{i=1}^{n}(yi-\hat{y}i)^2}{\sum_{i=1}^{n}(yi-\hat{y})^2} \quad \text{.....(12)}$$

where y_i represents observed values, $\hat{y}i$ denotes predicted values, $\hat{y}$ indicates the mean observed value, and n represents the total number of observations.

Finally, SHAP-based explainability analysis was conducted to quantify the contribution of individual physicochemical and heavy metal parameters to WQI predictions and to interpret model behavior in terms of feature importance, directionality, and impact on prediction outcomes.

3.8 GIS-Based Spatial Analysis

GIS-based spatial analysis was conducted to examine the spatial distribution and variation of river water quality parameters across the study area. Geographic coordinates of all sampling locations were collected using GPS and processed in ArcGIS 10.8 software to generate spatial distribution maps for the WQI, physicochemical parameters, heavy metals, and clustering outputs.

Spatial interpolation was performed using the IDW method to estimate water quality conditions at unsampled locations. The IDW approach assigns greater influence to nearby observations, making it suitable for modeling spatially continuous environmental variables. A power parameter of 2 was applied to control the rate of distance decay, and a spatial resolution of 30 m × 30 m was used for raster generation to ensure consistent spatial representation. All spatial analyses were conducted under the World Geodetic System 1984 (WGS 84) coordinate reference system. The IDW interpolation model is expressed in **Equation 13**.

$$Z(x_0)=\frac{\sum_{i=1}^{n}\frac{Z(Xi)}{dp}}{\sum_{i-1}^{n}\frac{1}{dp}} \quad \text{.....(13)}$$

where $Z(x_0)$ represents the estimated value at an unsampled location, $Z(x_i)$ denotes observed values at sampled locations, d is the distance between sampled and unsampled points, and p is the power parameter.

4. Results and Discussions

4.1 Clustering-Based Exploratory Analysis

4.1.1 Anomaly Detection

The anomaly detection results obtained using the One-Class Support Vector Machine (SVM) are presented in **Figure 3**. Most observations were classified as normal, while a limited number of data points were identified as anomalies and are highlighted by red markers. These anomalous observations are distributed across both high and low WQI ranges, indicating substantial deviations from the dominant water quality patterns.

The dataset contains 7,616 observations from the Turag, Balu, Shitalakshya, and Buriganga rivers collected between 2020 and 2024. Given the substantial spatial and temporal variability caused by industrial discharge, municipal wastewater, agricultural runoff, and seasonal hydrological changes, the presence of anomalies is expected. These anomalies likely represent unusual environmental conditions, localized pollution events, sudden contaminant inputs, or extreme water quality states that deviate from normal patterns. Identifying such observations is important for detecting potential pollution incidents and enhancing the reliability of clustering and predictive modeling, thereby enabling a more robust assessment of water quality dynamics across the study area.

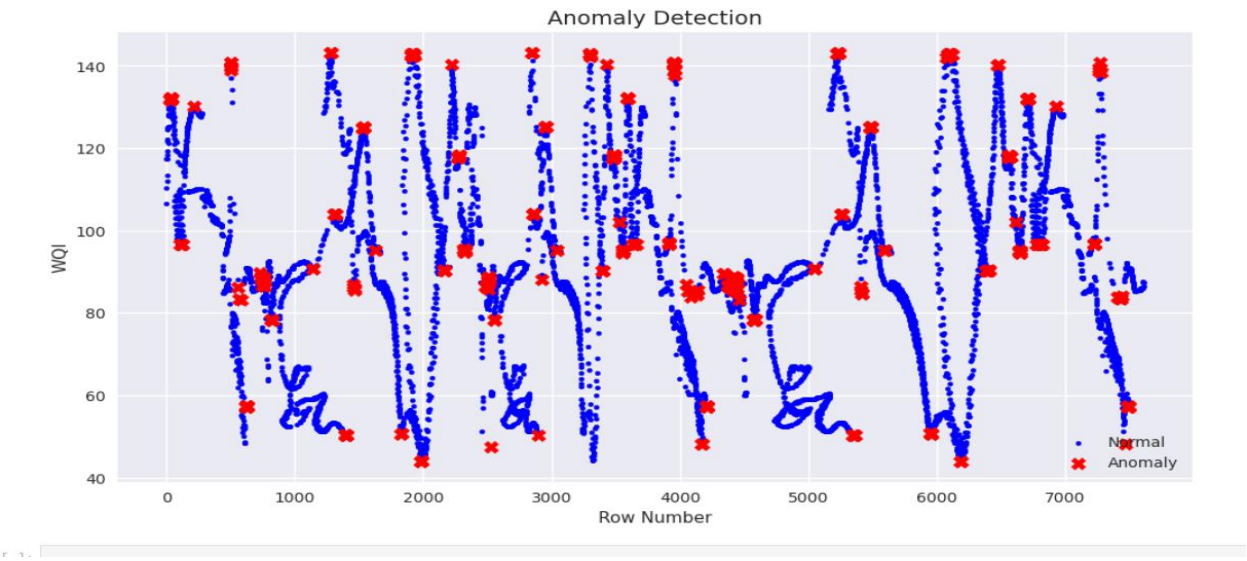


Figure 3. Anomaly Detection using the One-Class SVM for WQI

4.2 Model Performance

Table 3 presents the comparative performance of the three deep learning models used for WQI prediction. Among the evaluated models, the LSTM demonstrates the best predictive performance on the test dataset. It achieves the highest $R^2 = 0.99$, indicating that the model can explain approximately 99% of the variance in WQI values. In addition, the LSTM records the lowest error values, with an MSE of 0.0095, RMSE of 0.0776, and MAE of 0.0567, reflecting its strong capability to capture temporal dependencies and nonlinear relationships in sequential environmental data.

Table 3. DL Model Performance

Environmental Parameters	Model	R^2	MSE	RMSE	MAE
WQI	ANN	0.96	0.0371	0.1927	0.1644
	LSTM	0.9903	0.0095	0.0776	0.0567
	Bi-LSTM	0.65	0.3186	0.5645	0.3559

The ANN model also shows satisfactory predictive capability, achieving an R^2 value of 0.96 with moderate error values (MSE: 0.0371, RMSE: 0.1927, and MAE: 0.1644). Although the ANN performs reasonably well, its performance is slightly inferior to that of the LSTM due to its limited ability to effectively model sequential temporal patterns in environmental parameters. In contrast, the Bi-LSTM model exhibits the weakest predictive performance among the three models. It records the lowest R^2 value of 0.65 along with the highest error values (MSE: 0.3186, RMSE: 0.5645, and MAE: 0.3559). The lower predictive performance of the Bi-LSTM model suggests that the dataset may not contain sufficiently strong bidirectional temporal dependencies, while the increased architectural complexity may have contributed to overfitting and reduced generalization capability. Despite the bidirectional architecture being theoretically advantageous for sequence learning, the results indicate that the Bi-LSTM model was less effective under the given dataset and feature configuration.

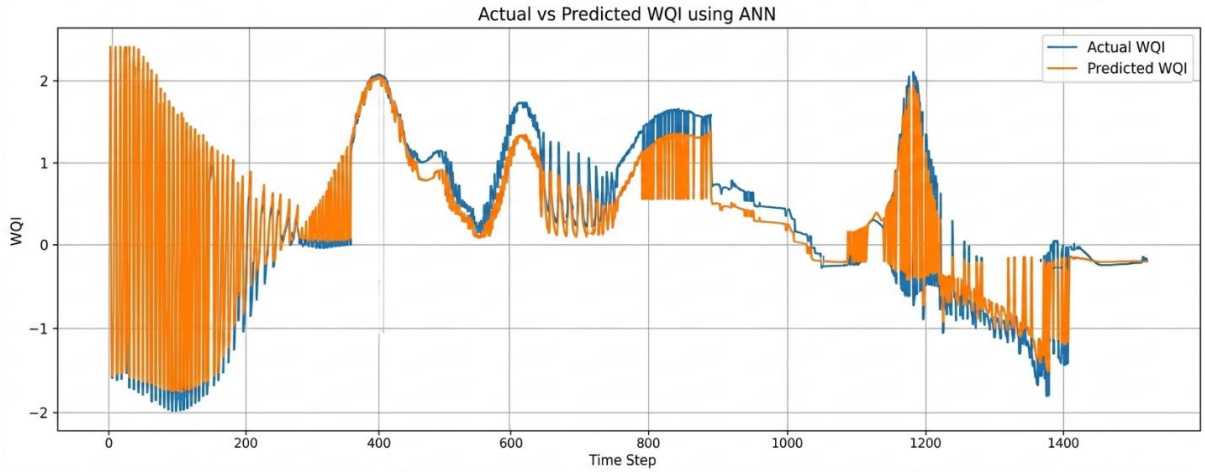
Overall, the results indicate that temporal modeling plays a crucial role in accurate WQI forecasting. The LSTM model outperforms both ANN and Bi-LSTM architectures, making it the most suitable approach for predicting water quality variations in the present study.

4.3 Visual Analysis of Prediction Accuracy

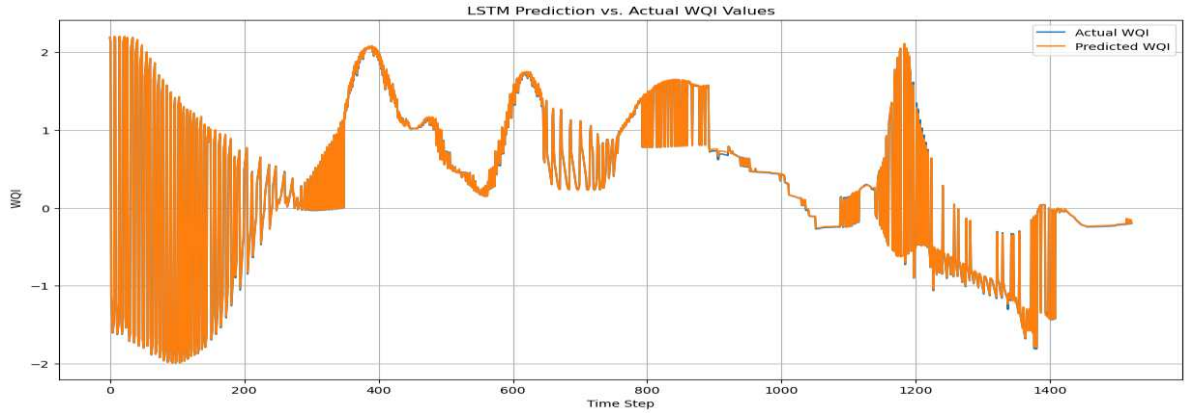
To complement the quantitative evaluation, **Figure 4(a-c)** presents the comparison between actual and predicted WQI values for the ANN, LSTM, and Bi-LSTM models. The visual analysis provides a clearer understanding of each model's ability to capture temporal variations, nonlinear fluctuations, and overall WQI trends across the time sequence.

4.3.1. Artificial Neural Network (ANN)

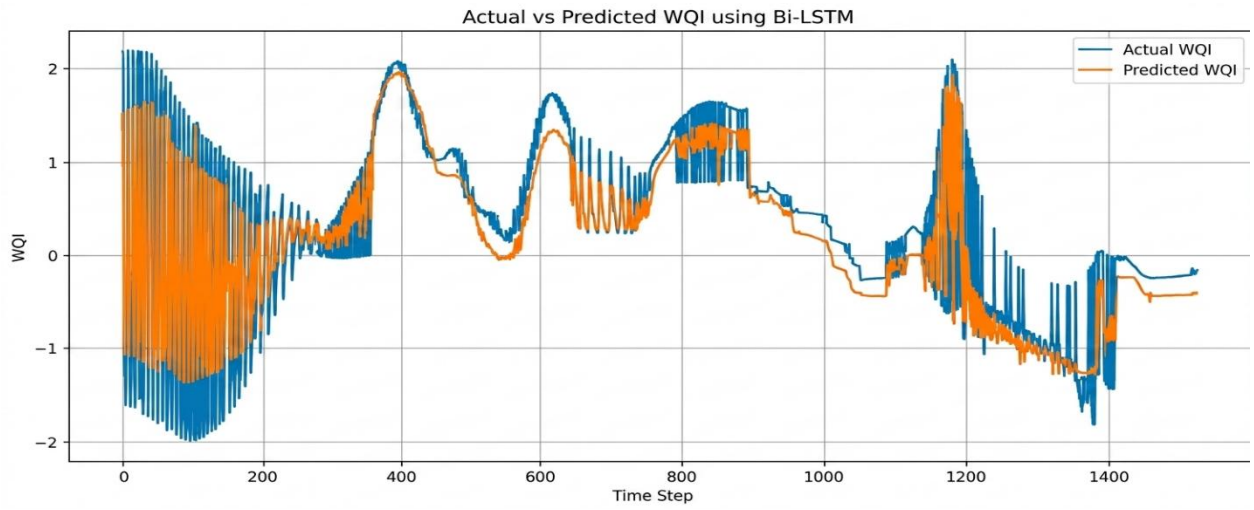
The ANN model generally follows the overall WQI trend but shows noticeable deviations during abrupt fluctuations and peak variations. The predicted curve appears comparatively smoother than the observed sequence, indicating limited capability in capturing complex temporal patterns. These observations are consistent with the moderate predictive performance of the ANN model obtained during quantitative evaluation.



a



b



c

Figure 4(a-c). Actual versus predicted WQI for all models

4.3.2. Long Short-Term Memory (LSTM)

The LSTM model exhibits strong agreement between actual and predicted WQI values across most time steps. The model effectively captures both gradual trends and short-term fluctuations with minimal prediction deviations. Minor discrepancies are observed only during sudden spikes, where the predicted sequence slightly smooths extreme variations. Overall, the visual consistency supports the superior predictive performance of the LSTM model.

4.3.3. Bidirectional Long Short-Term Memory (Bi-LSTM)

The Bi-LSTM model captures the general WQI trend but demonstrates larger deviations during abrupt fluctuations and highly dynamic regions. The predicted sequence appears comparatively over-smoothed and less aligned with the observed data than the standard LSTM model. This behavior indicates comparatively weaker generalization capability and reduced predictive stability for the present dataset.

4.4 Analysis of Training and Validation Loss Dynamics

The learning curves of the ANN, LSTM, and Bi-LSTM models, shown in **Figure 5(a-c)**, provide important insights into their convergence behavior, training stability, and generalization capability during the learning process. In general, an effective model exhibits a rapid reduction in both

training and validation losses during the initial epochs, followed by stable convergence with a relatively small gap between the two curves, indicating strong predictive generalization without severe overfitting.

4.4.1. Artificial Neural Network (ANN)

The ANN model shows a rapid initial decrease in both training and validation losses during the early epochs, reflecting efficient early-stage learning. The training loss steadily declines and stabilizes at a relatively low value toward the later epochs. The validation loss also decreases initially but exhibits moderate fluctuations after convergence, particularly in the later training stages. Despite these variations, the validation curve remains reasonably close to the training curve, indicating that the ANN model does not suffer from severe overfitting. However, the comparatively larger fluctuations and slightly wider gap between the training and validation losses suggest weaker generalization capability relative to the LSTM model. These observations are consistent with the ANN's comparatively lower predictive accuracy in WQI forecasting.

4.4.2. Long Short-Term Memory (LSTM)

The LSTM model demonstrates stable and efficient convergence throughout the training process. The training loss gradually decreases from approximately 0.00007 to below 0.00004 over the training epochs, indicating continuous learning and optimization of temporal patterns within the WQI dataset. Similarly, the validation loss remains relatively low and closely follows the training curve for most epochs, suggesting good generalization capability. Although a temporary spike in validation loss is observed around epoch 13, the model quickly stabilizes afterward without sustained divergence between the training and validation curves. The small gap between the two losses and the smooth convergence behavior confirm that the LSTM model effectively learns sequential dependencies while maintaining stable predictive performance.

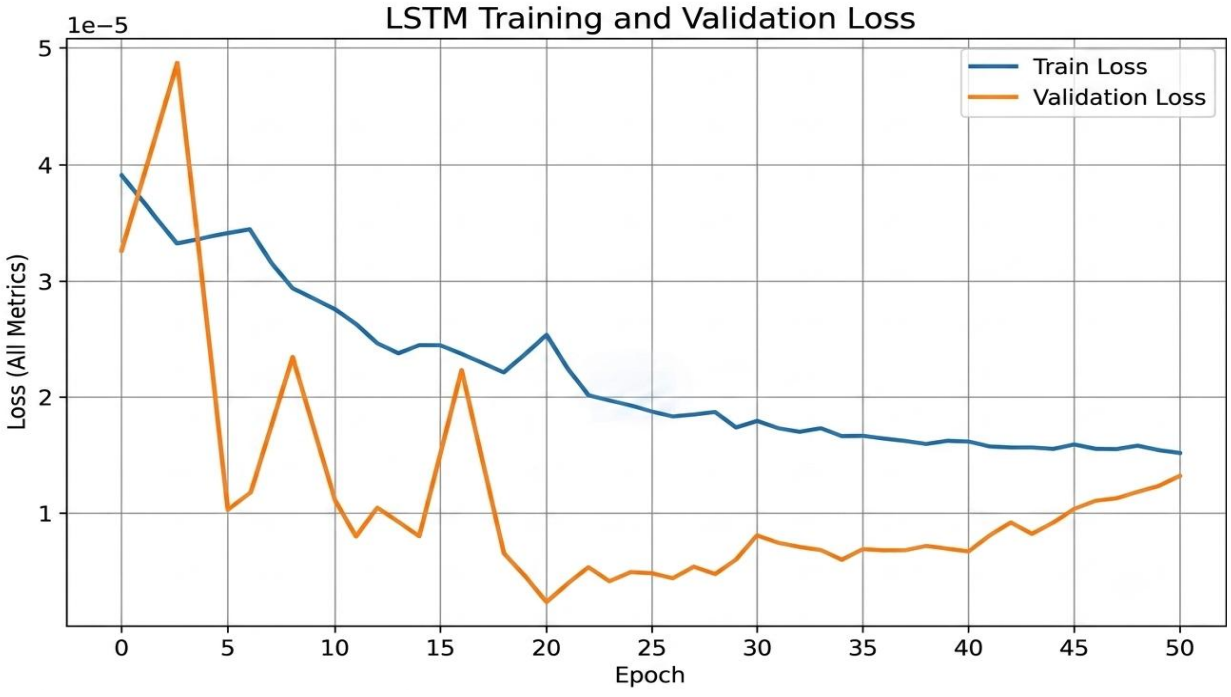
4.4.3. Bidirectional Long Short-Term Memory (Bi-LSTM)

The Bi-LSTM model exhibits a gradual reduction in training loss throughout the learning process, indicating that the model successfully learns temporal features from the sequential WQI data. The validation loss also decreases significantly during the initial epochs before stabilizing at a relatively constant level. However, a noticeable gap persists between the training and validation loss curves during later epochs, suggesting reduced generalization performance compared to the standard LSTM model. In addition, the validation loss demonstrates moderate oscillations,

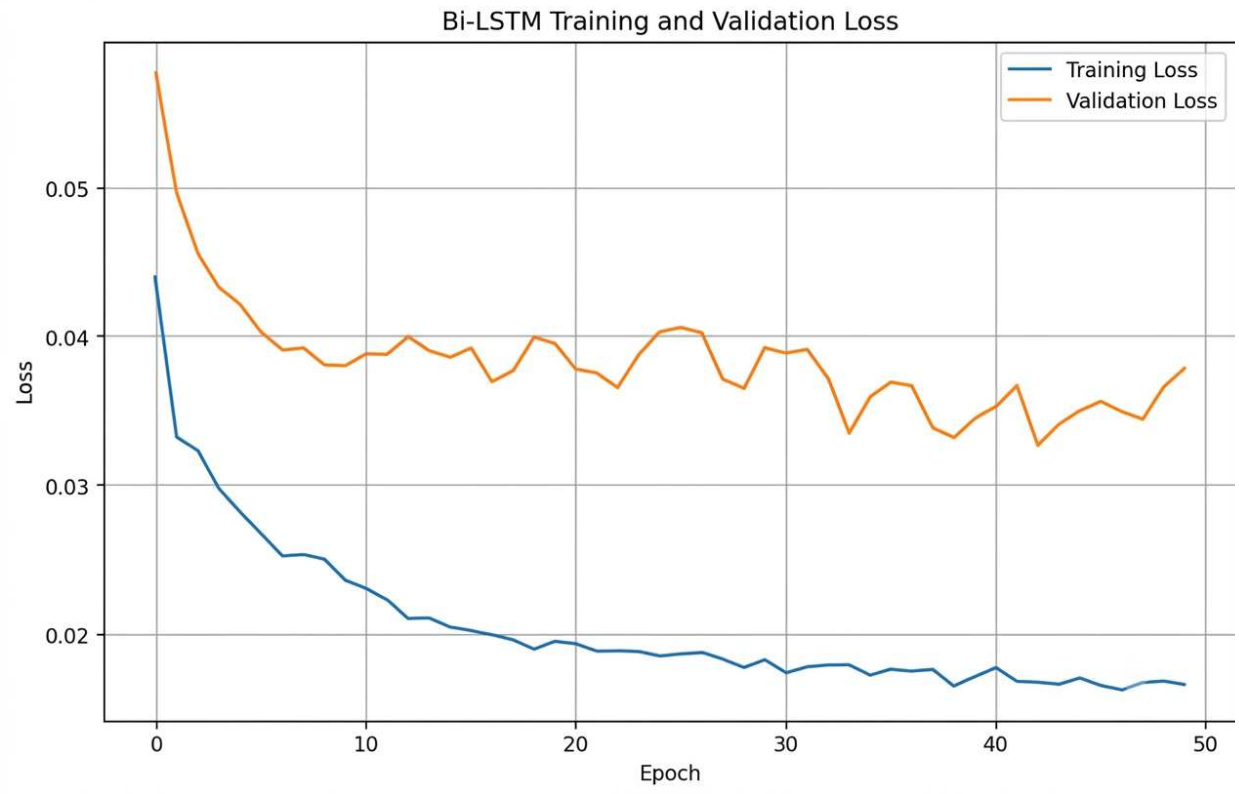
indicating instability in the model's validation performance. This behavior may be attributed to the increased architectural complexity of the Bi-LSTM network, which can increase the risk of overfitting when the dataset does not contain sufficiently strong bidirectional temporal dependencies. Consequently, although the Bi-LSTM model achieves convergence, its training dynamics indicate comparatively weaker predictive stability and generalization capability for the present WQI forecasting task.



a



b



c

Figure 5(a-c). Training and Validation Loss of all models

4.5 SHAP-Based Feature Importance Analysis

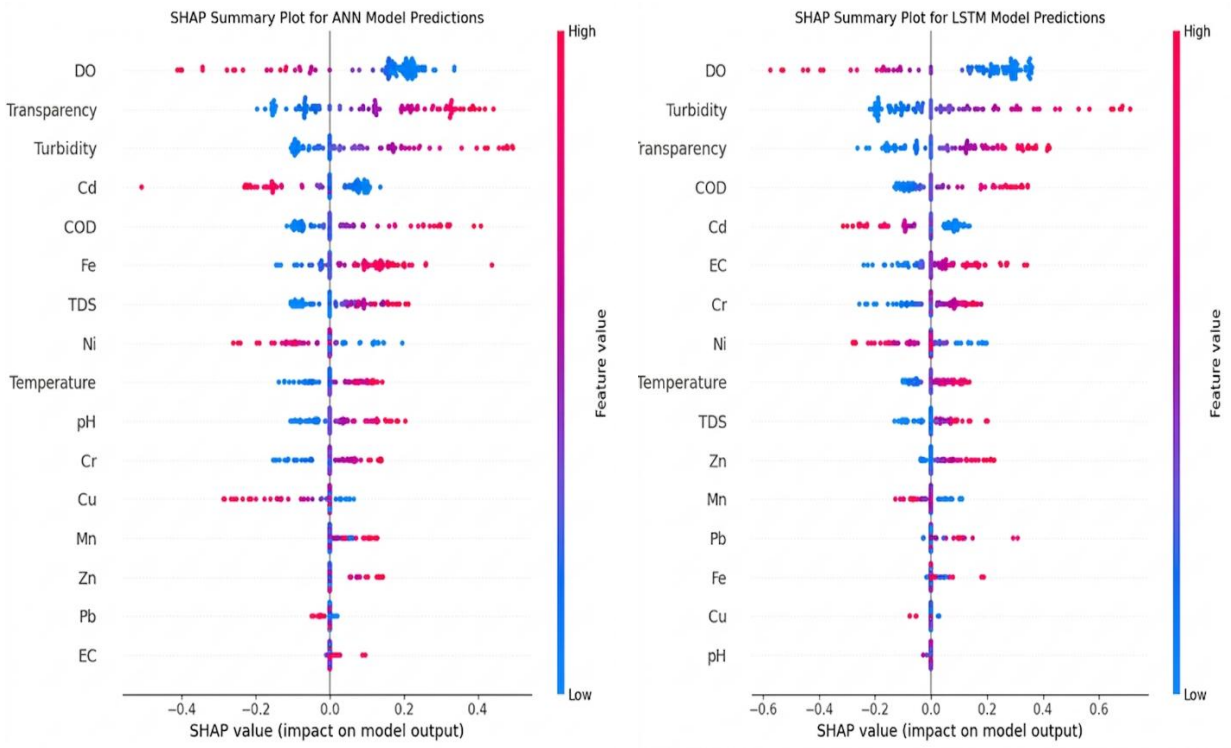
The SHAP analysis across the ANN, LSTM, and Bi-LSTM models (**Figure 6(a-c)**) reveals both common patterns and model-specific variations in the factors influencing WQI prediction. Across all three architectures, DO consistently emerges as the most influential parameter, highlighting its critical role in determining river water quality conditions. Transparency-related variables also demonstrate strong importance, indicating the influence of water clarity and suspended particle dynamics on WQI estimation. Heavy metal and contamination-related parameters such as Cd, Cr, Ni, and EC further show notable contributions, confirming the importance of pollutant concentration in influencing water quality variation.

The influence of individual parameters varies among the models. The LSTM model exhibits broader and more stable SHAP distributions, indicating its superior capability in capturing temporal and nonlinear interactions among environmental variables. In contrast, the ANN model shows comparatively compressed SHAP distributions, suggesting limited capability in modeling sequential dependencies and reduced variability in feature contribution patterns. The Bi-LSTM

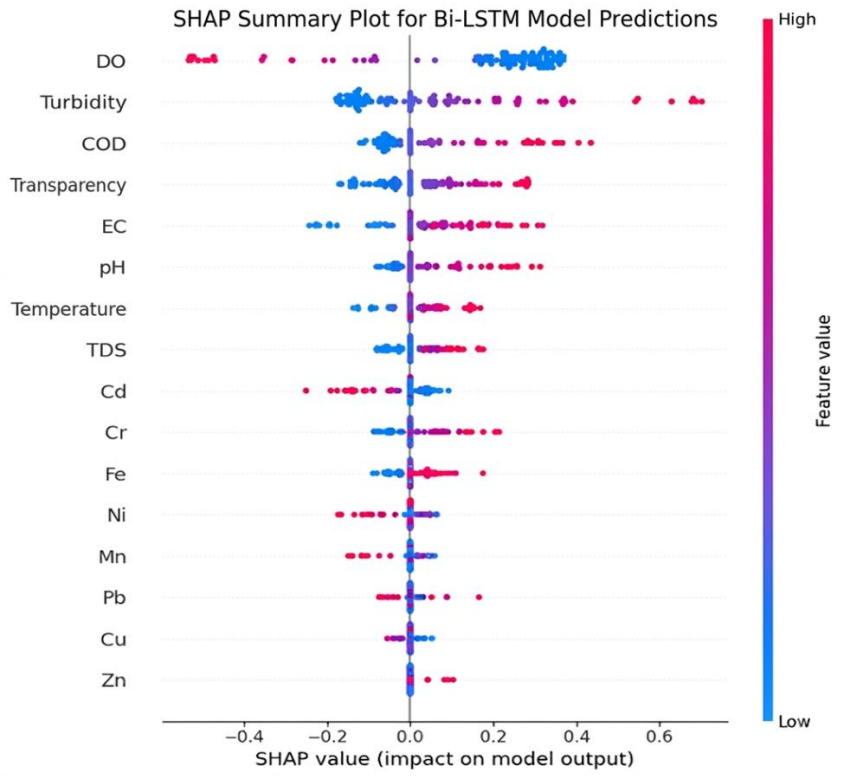
model captures a wider range of environmental interactions than the ANN; however, its SHAP values appear more scattered and less consistent compared to the LSTM model, reflecting comparatively weaker predictive stability and generalization performance.

Among physicochemical parameters, turbidity, TDS, EC, and transparency demonstrate moderate-to-high contributions due to their direct relationship with suspended particles and dissolved pollutant concentrations. Temperature-related variables show relatively stronger importance in the ANN model, whereas turbidity and EC exhibit higher influence within the Bi-LSTM architecture. In contrast, Pb, Cu, and Zn consistently show lower SHAP contributions across all models, indicating comparatively weaker influence on WQI prediction within the present dataset.

Overall, the SHAP results confirm that dissolved oxygen, transparency, dissolved solids, and contamination-related variables are the dominant drivers of WQI prediction, although their relative importance varies among model architectures. The consistency of key feature importance patterns across ANN, LSTM, and Bi-LSTM models further supports the robustness and reliability of the proposed AI-based framework for intelligent water quality assessment and environmental monitoring.



a **b**



c

Figure 6(a-c). SHAP diagram of all models

4.6 GIS Mapping

The spatial distribution maps of physicochemical parameters and heavy metal concentrations collected from different river sampling locations are presented in **Figures 7(a-h)** and **8(a-h)**. Overall, the river system exhibits noticeable spatial variability in water quality conditions, reflecting the influence of both natural processes and anthropogenic activities along different river stretches.

The physicochemical parameter maps shown in **Figure 7(a-h)** indicate relatively stable but spatially heterogeneous water quality conditions across the river network. The pH values (**Figure 7(a)**) range from 7.05 to 8.62, indicating predominantly neutral to slightly alkaline conditions suitable for aquatic ecosystems. Slightly lower pH values are observed in localized downstream sections, which may be associated with increased pollutant discharge or organic decomposition. TDS concentrations (**Figure 7(b)**) vary from 0.35 to 10.39 mg/L, with elevated concentrations observed in several central and downstream segments, suggesting increased dissolved mineral and pollutant loading. Temperature distribution (**Figure 7(c)**) remains comparatively stable throughout

the river system, ranging from 21.44 °C to 32.12 °C, indicating limited thermal variation across sampling locations. Transparency levels (**Figure 7(d)**) show considerable spatial variation, ranging from 1.25 to 28.66 inches. Lower transparency in several river sections indicates higher suspended particle concentration and reduced water clarity. Turbidity values (**Figure 7(e)**) vary substantially from 18.45 to 1513.06 mg/L, with highly elevated concentrations in downstream and densely connected river segments, reflecting strong sediment transport and suspended solid accumulation. Similarly, COD concentrations (**Figure 7(f)**) range from 24.31 to 2549.25 mg/L, indicating severe organic pollution in several localized regions, likely associated with untreated wastewater discharge and anthropogenic activities. DO concentrations shown in **Figure 7(g)** range from near-zero values to 22.81 mg/L, demonstrating substantial variability in oxygen availability across the river system. Lower DO concentrations in several river stretches indicate elevated microbial activity and organic pollution stress. EC values (**Figure 7(h)**) range from 45.36 to 2533.96 mg/L, with higher conductivity observed in polluted downstream sections, suggesting increased dissolved ion and salt concentrations due to runoff and contamination sources.

The heavy metal distribution maps presented in **Figure 8(a-h)** further reveal significant spatial variability in contamination levels throughout the river network. Cd concentrations range from 0.0006 to 0.0595 mg/L, while Cr concentrations vary from 0.1069 to 0.4700 mg/L, with elevated values concentrated in several downstream and urbanized sections. Cu and Fe concentrations also exhibit localized hotspots, indicating possible industrial, municipal, or surface runoff contributions. Mn, Ni, Pb, and Zn similarly demonstrate spatially heterogeneous distributions, with higher concentrations generally observed in downstream regions and areas influenced by anthropogenic activities.

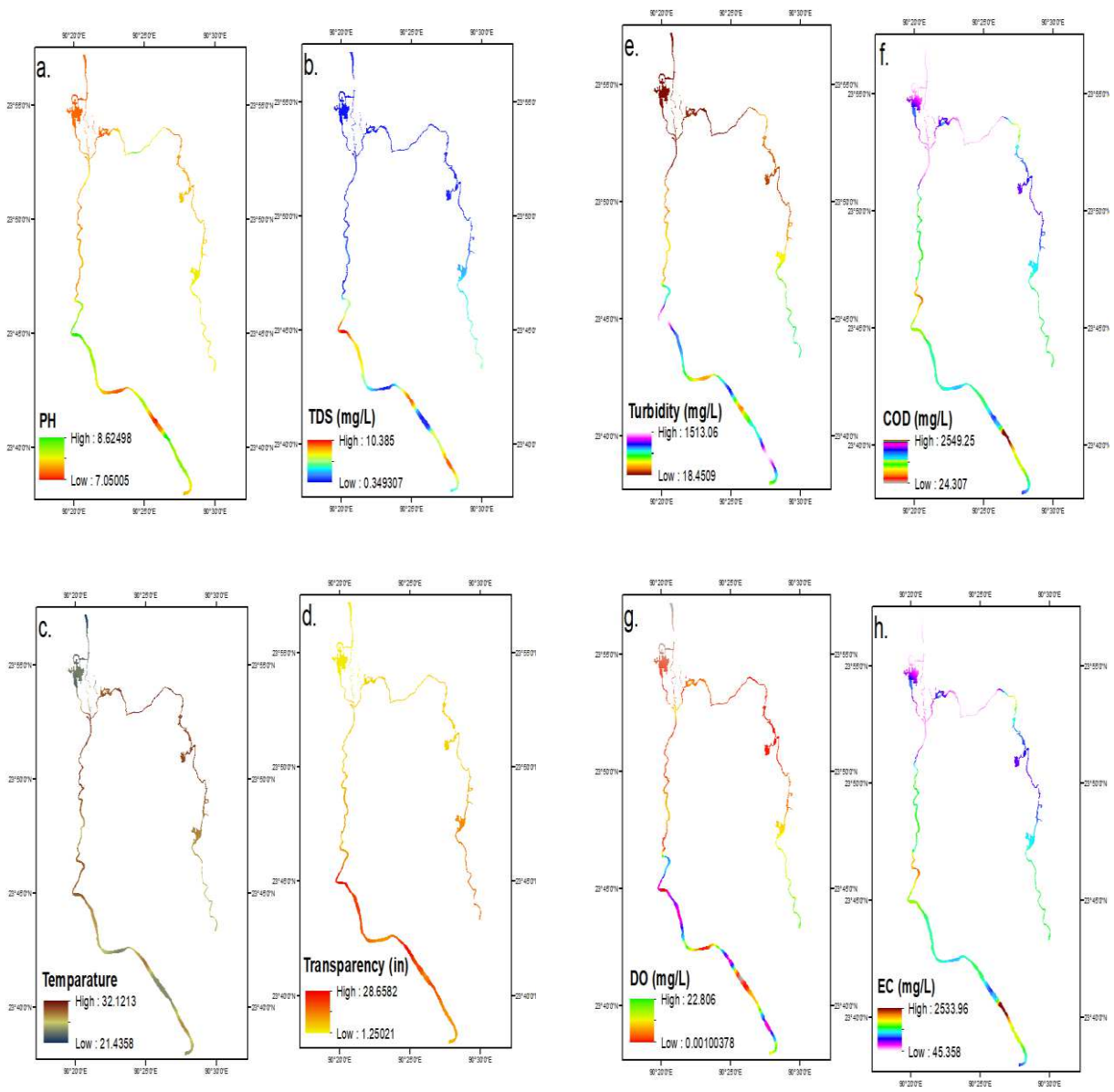


Figure 7(a-h). Spatial variation of physicochemical parameters

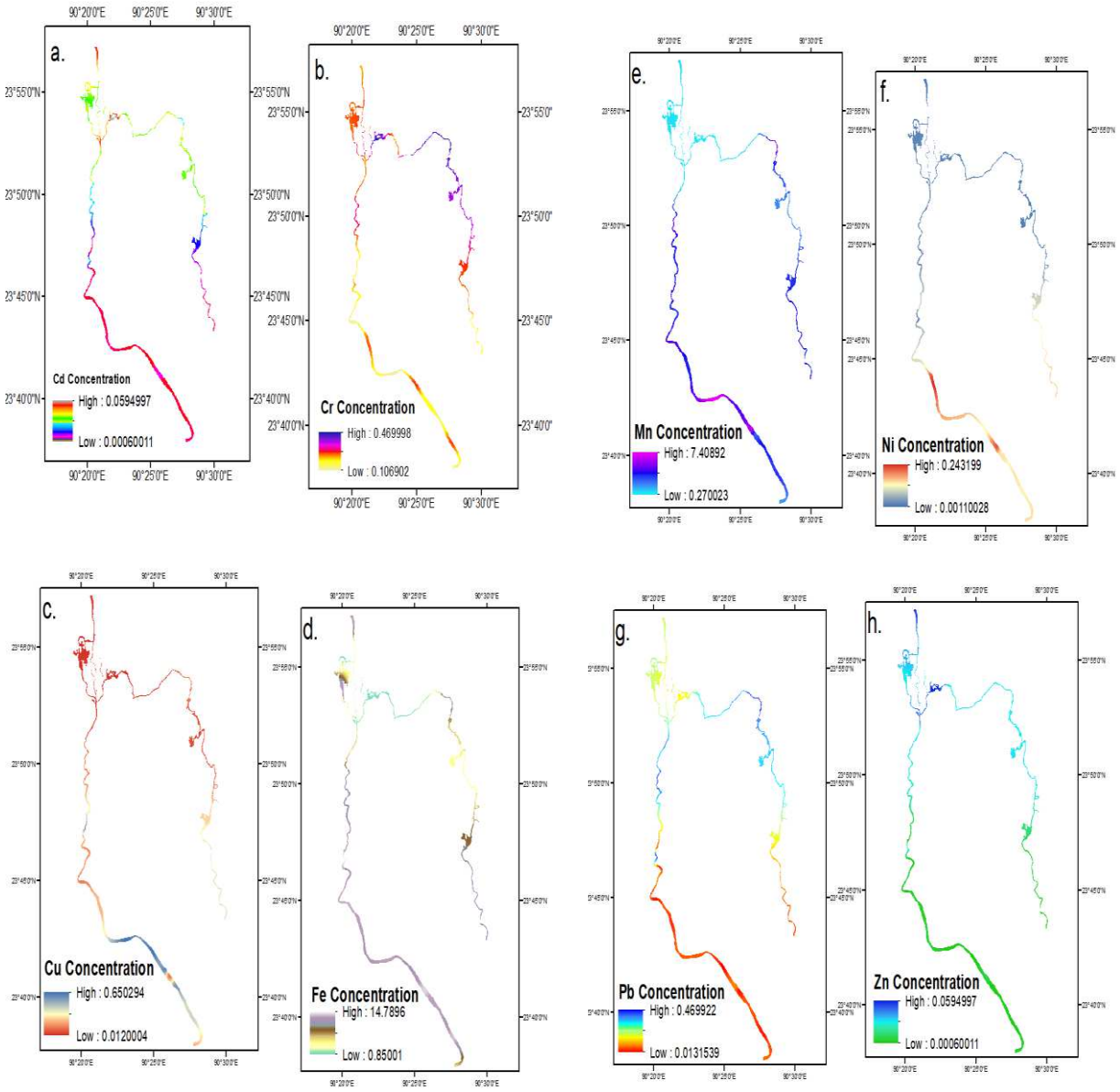


Figure 8(a-h). Spatial variation of heavy metal parameters

538

539 Overall, the spatial distribution patterns demonstrate that water quality deterioration is more
540 pronounced in downstream and densely impacted river sections, where elevated physicochemical
541 pollution indicators coexist with increased heavy metal contamination. These findings highlight
542 the combined effects of sediment transport, organic pollution, dissolved contaminants, and
543 anthropogenic discharge on river water quality conditions. The observed spatial variability

emphasizes the importance of continuous monitoring and location-specific management strategies for sustainable river ecosystem protection and pollution control.

5. Co-elaborative Discussion

The findings of this study directly address the methodological gap identified in the literature review, where previous studies mainly relied on conventional statistical analysis, standalone ML models, or isolated GIS-based assessments. Earlier work using regression and correlation analysis provided useful relationships among water quality parameters, but remained limited in capturing nonlinear and complex pollution dynamics (Sharmaa & Panditb). Similarly, time-series and data-mining approaches improved pollution trend prediction but were often restricted to single-parameter forecasting, such as total phosphorus prediction, without integrated WQI assessment, SHAP interpretation, clustering, or GIS-based hotspot mapping (Ma & Chen, 2025). In contrast, the present study developed a unified framework that integrates preprocessing, WQI calculation, anomaly detection, ANN, LSTM, Bi-LSTM prediction, SHAP explainability, and GIS-IDW spatial mapping. Therefore, the present findings fill the gap by providing a combined predictive, interpretable, and spatially explicit framework for assessing highly polluted urban river systems.

The model performance results also fill the gap related to the limited use of advanced DL architectures for multi-parameter WQI prediction in Dhaka's rivers. Studies by (Nishat et al., 2025) compared several ML models for WQI prediction in urban rivers of Dhaka and reported strong performance from ANN and RF, but their study was limited by a smaller sample size, fewer water quality parameters, and the absence of LSTM, Bi-LSTM, SHAP, GIS-IDW, clustering, and extensive heavy metal analysis. Another study by (Karbasi et al., 2024) demonstrated the usefulness of sequential learning through a Boruta-XGB-CNN-LSTM framework, but their work focused only on EC forecasting rather than integrated WQI prediction. In the present study, the LSTM model achieved the best predictive performance, with $R^2 = 0.9903$, MSE = 0.0095, RMSE = 0.0776, and MAE = 0.0567. This result shows that LSTM can effectively capture nonlinear and sequential relationships among physicochemical and heavy metal parameters, thereby extending previous WQI prediction studies from standalone machine learning toward DL-based multi-parameter river water quality assessment.

The SHAP-based results fill another important gap related to the limited interpretability of AI and DL models in water quality research. Although studies by (Zhang et al., 2025) applied SHAP to identify dominant pollution indicators in groundwater quality assessment, their study did not focus on urban river WQI prediction or integrate GIS-IDW mapping, clustering, and comparative ANN, LSTM and Bi-LSTM modeling. In the present study, SHAP analysis identified DO, turbidity, transparency, and COD as the most influential variables controlling WQI prediction. These findings improve model transparency by showing not only how accurately the model predicts WQI but also which environmental parameters drive the prediction. As a result, the study advances previous DL-based water quality research by linking prediction accuracy with explainable environmental interpretation, making the model outputs more useful for pollution monitoring, parameter prioritization, and river management decision-making.

The clustering and GIS-based findings further address the spatial assessment gap highlighted in earlier studies on the Turag, Balu, Shitalakshya, and Buriganga Rivers. Studies by (Khan et al., 2020) examined heavy metals and PAHs in Turag River sediments, but their work focused on sediment contamination rather than WQI prediction, clustering, SHAP, or GIS-IDW-based spatial assessment. Another study by (Rony et al., 2025) applied GIS and WQI analysis to assess river pollution around Dhaka, but the study was limited by restricted parameters and did not include deep learning, SHAP, clustering, or heavy metal-based predictive modeling. Another study by (Suchi et al., 2024) reported heavy metal contamination and associated ecological and health risks in Dhaka's river systems, but their study was constrained by limited spatial and seasonal coverage. The present study fills these gaps by using anomaly detection to identify pollution groupings and applying GIS-IDW interpolation to map spatial pollution hotspots across four major urban rivers. Therefore, the findings provide a more comprehensive decision-support framework that explains pollution patterns, identifies vulnerable zones, and supports targeted river pollution management.

6. Conclusion

This study presents a comprehensive assessment of water quality conditions in the Turag, Balu, Shitalakshya, and Buriganga Rivers through the integration of DL and GIS. By analyzing 7,616 datasets collected during the 2024 monsoon season, the research identified the dominant physicochemical and heavy metal parameters influencing the WQI and developed a predictive

framework for urban river water quality assessment. The study also examined spatial pollution variability and hotspot distributions across the river systems to support sustainable water resource management in densely populated and industrialized regions of Dhaka.

The findings demonstrated that parameters such as DO, turbidity, transparency, EC, and heavy metals including Cd, Cr, Ni, and Pb significantly influence WQI prediction. Among the developed DL models, the LSTM achieved the highest predictive accuracy and strongest generalization capability, outperforming ANN and Bi-LSTM models. SHAP analysis provided interpretable insights into feature importance and revealed the dominant environmental drivers affecting water quality conditions. In addition, GIS-based IDW spatial mapping effectively identified pollution hotspot regions and highlighted severe contamination associated with industrial discharge, urban runoff, and untreated municipal wastewater across the studied rivers.

Despite these findings, the study was limited to monsoon-season observations and depended on available monitoring data, which may influence long-term model generalizability. Future research should incorporate multi-seasonal datasets, real-time sensor monitoring, satellite observations, and advanced hybrid DL frameworks to improve prediction reliability and temporal coverage. The integration of scalable DL-GIS systems can contribute to early-warning mechanisms, pollution control strategies, and sustainable urban river management for rapidly developing cities.

Acknowledgements

We thank the Department of Civil Engineering at IUBAT – International University of Business Agriculture and Technology for supporting this research work.

Funding Declaration

No funding was received for conducting this study.

Author contribution

Md. Sojib Sheikh: Writing – original draft, Conceptualization, Data curation, Formal analysis, Investigation, Methodology, Resources, Software, Validation, Visualization. **Md. Hasan:** Writing – original draft, Conceptualization, Data curation, Formal analysis, Investigation, Methodology, Resources, Software, Validation, Visualization. **Bishwajit Chandra Mazumdar:** Writing –

review & editing, Conceptualization, Data curation, Formal analysis. **Mohammad Nyme Uddin:** Writing – review & editing, Conceptualization, Project administration, Supervision.

Declaration of generative AI

In preparing this work, the author employed pre-trained large language models to assist with grammar checking and to improve the manuscript's clarity. Afterward, the author carefully reviewed and edited the text as needed and accepts full responsibility for the published content.

Conflict of Interest

The authors report no conflicts of interest.

Data Availability

Data can be obtained upon request from the first author.

Declaration of Competing Interest

The authors state that they have no known conflicts of interest or personal relationships that could have influenced the work presented in this paper.

Ethical approval

Not applicable

Clinical trial number

Not applicable

References

Ahamad, F., & Singh, V. K. (2025). AI-Driven Predictive Modeling for Real-Time Water Quality Monitoring in Urban Water Supply Systems. *Int. J. Sci. Res. Sci. Eng. Technol*, *12*(2), 838–849.

Ahmed, S. F., Alam, M. S. B., Hassan, M., Rozbu, M. R., Ishtiak, T., Rafa, N., Mofijur, M., Shawkat Ali, A., & Gandomi, A. H. (2023). Deep learning modelling techniques: current progress, applications, advantages, and challenges. *Artificial Intelligence Review*, *56*(11), 13521–13617.

Ahmed, U., Mumtaz, R., Anwar, H., Mumtaz, S., & Qamar, A. M. (2020). Water quality monitoring: from conventional to emerging technologies. *Water Supply*, *20*(1), 28–45.

Apandi, N. M., Mohamed, R. M. S. R., Al-Gheethi, A., & Kassim, A. H. M. (2019). Microalgal biomass production through phycoremediation of fresh market wastewater and potential applications as aquaculture feeds. *Environmental Science and Pollution Research*, *26*(4), 3226–3242.

Association, A. P. H., Association, A. W. W., Federation, W. P. C., & Federation, W. E. (1905). *Standard Methods for the Examination of Water and Wastewater: Including Bottom Sediment and Sludges* (Vol. 1). American public health association.

Gavrilaș, S., Burescu, F.-L., Chereji, B.-D., & Munteanu, F.-D. (2025). The impact of anthropogenic activities on the catchment's water quality parameters. *Water*, *17*(12), 1791.

Hoque, S. F., Peters, R., Whitehead, P., Hope, R., & Hossain, M. A. (2021). River pollution and social inequalities in Dhaka, Bangladesh. *Environmental Research Communications*, *3*(9), 095003.

Islam, M. M., Rahman, M., Nargis, S., Ahamed, M. R., Mollik, R. S., Boby, N. J. K., Raju, M. R., Proshad, R., & Aziz, M. A. (2023). Elevating health of the Turag River: a synergistic water quality assessment approach. *Earth Systems and Environment*, *7*(4), 761–780.

Iwar, R. T., Utsev, J. T., & Hassan, M. (2021). Assessment of heavy metal and physico-chemical pollution loadings of River Benue water at Makurdi using water quality index (WQI) and multivariate statistics. *Applied Water Science*, *11*(7), 124.

Karbasi, M., Ali, M., Bateni, S. M., Jun, C., Jamei, M., Farooque, A. A., & Yaseen, Z. M. (2024). Multi-step ahead forecasting of electrical conductivity in rivers by using a hybrid Convolutional Neural Network-Long Short-Term Memory (CNN-LSTM) model enhanced by Boruta-XGBoost feature selection algorithm. *Scientific reports*, *14*(1), 15051.

Kazemi, U., & Soleimani, S. (2025). A new approach data processing: density-based spatial clustering of applications with noise (DBSCAN) clustering using game-theory: U. Kazemi, S. Soleimani. *Soft Computing*, *29*(3), 1331–1346.

Khan, R., Islam, M. S., Tareq, A. R. M., Naher, K., Islam, A. R. M. T., Habib, M. A., Siddique, M. A. B., Islam, M. A., Das, S., & Rashid, M. B. (2020). Distribution, sources and ecological risk of trace elements and polycyclic aromatic hydrocarbons in sediments from

a polluted urban river in central Bangladesh. *Environmental Nanotechnology, Monitoring & Management*, *14*, 100318.

Khosravi, K., Farooque, A. A., Karbasi, M., Ali, M., Heddam, S., Faghfouri, A., & Abolfathi, S. (2025). Enhanced water quality prediction model using advanced hybridized resampling alternating tree-based and deep learning algorithms. *Environmental Science and Pollution Research*, *32*(11), 6405–6424.

Liu, J., Qiu, Z., Feng, J., Wong, K. P., Tsou, J. Y., Wang, Y., & Zhang, Y. (2023). Monitoring total suspended solids and chlorophyll-a concentrations in turbid waters: A case study of the Pearl River Estuary and coast using machine learning. *Remote Sensing*, *15*(23), 5559.

Ma, T., & Chen, X. (2025). Time Series Analysis for the Adaptive Prediction of Total Phosphorus in the Yangtze River: A Machine Learning Approach. *Water*, *17*(4), 603.

Manasa, R. L., & Mehta, A. (2020). Wastewater: sources of pollutants and its remediation. In *Environmental Biotechnology Vol. 2* (pp. 197–219). Springer.

Mellyzar, M., Hernani, H., Nahadi, N., & Agustina, S. (2025). Bibliometric Analysis of Water Pollution Research: Focus on Industry Impacts. *Jurnal Presipitasi: Media Komunikasi dan Pengembangan Teknik Lingkungan*.

Miah, O., Anik, A. H., Sorker, R., Parvin, F., Shammi, M., & Tareq, S. M. (2025). Impacts of rapid urbanization on long-term water quality of the peripheral River of Dhaka, Bangladesh. *Water Environment Research*, *97*(1), e70000.

Moeini, M., Shojaeizadeh, A., & Geza, M. (2021). Supervised machine learning for estimation of total suspended solids in urban watersheds. *Water*, *13*(2), 147.

Nishat, M. H., Khan, M. H. R. B., Ahmed, T., Hossain, S. N., Ahsan, A., El-Sergany, M., Shafiquzzaman, M., Imteaz, M. A., & Alresheedi, M. T. (2025). Comparative analysis of machine learning models for predicting water quality index in Dhaka's rivers of Bangladesh. *Environmental Sciences Europe*, *37*(1), 31.

Odong, T., Van Heerwaarden, J., Van Hintum, T., Van Eeuwijk, F., & Jansen, J. (2013). Improving hierarchical clustering of genotypic data via principal component analysis. *Crop Science*, *53*(4), 1546–1554.

Paepae, T., Bokoro, P. N., & Kyamakya, K. (2021). From fully physical to virtual sensing for water quality assessment: A comprehensive review of the relevant state-of-the-art. *Sensors*, *21*(21), 6971.

Parvin, F., Haque, M. M., & Tareq, S. M. (2022). Recent status of water quality in Bangladesh: a systematic review, meta-analysis and health risk assessment. *Environmental challenges*, *6*, 100416.

Rony, M. M. H., Islam, M. T., Muyen, Z., Godhuli, M., Sultana, M. N., & Adham, A. (2025). GIS-based evaluation of pollution sources and water quality status in the Turag River, Bangladesh. *The Global Environmental Engineers*, *12*, 5–21.

Sarker, B., Keya, K. N., Mahir, F. I., Nahiun, K. M., Shahida, S., & Khan, R. A. (2021). Surface and ground water pollution: causes and effects of urbanization and industrialization in South Asia. *Scientific Review*, *7*(3), 32–41.

Sekarlangit, S., Widodo, C., & Tarno, T. (2024). A Comparison of Artificial Neural Network (ANN) and Long Short-Term Memory (LSTM) in River Water Quality Prediction. *International Journal of Current Science Research and Review*, *7*(4), 2000–2005.

Sharmaa, S., & Panditb, V. Correlation Study and Regression Analysis of Water Quality of Chhoiya River (a tributary of river Ganga) in Bijnor District (UP, India).

Subramanian, A., & Baskar, S. (2022). Water quality assessment of Noyyal river using water quality index (WQI) and multivariate statistical techniques. *Water Science*, *36*(1), 85–98.

Suchi, P. D., Shaikh, M. A. A., Saha, B., Moniruzzaman, M., Hossain, M. K., Parvin, A., & Parvin, A. (2024). Comprehensive index analysis approach for ecological and human health risk assessment of a tributary river in Bangladesh. *Heliyon*, *10*(13).

Torres-Vera, M.-A. (2023). Mapping of total suspended solids using Landsat imagery and machine learning. *International Journal of Environmental Science and Technology*, *20*(11), 11877–11890.

Uddin, M. A., Begum, M. S., Ashraf, M., Azad, A. K., Adhikary, A. C., & Hossain, M. S. (2023). Water and chemical consumption in the textile processing industry of Bangladesh. *PLOS Sustainability and Transformation*, *2*(7), e0000072.

van den Broeke, J., Carswell, L., Cade, L., Rosen, J., & Swartz, C. (2013). A Compendium of Sensors and Monitors and Their Use in the Global Water Industry.

Wan, X., Wang, W., Liu, J., & Tong, T. (2014). Estimating the sample mean and standard deviation from the sample size, median, range and/or interquartile range. *BMC medical research methodology*, *14*(1), 135.

Yin, H., Islam, M. S., & Ju, M. (2021). Urban river pollution in the densely populated city of Dhaka, Bangladesh: Big picture and rehabilitation experience from other developing countries. *Journal of Cleaner Production*, *321*, 129040.

Zhang, T., Wu, J., Chu, H., Liu, J., & Wang, G. (2025). Interpretable machine learning based quantification of the impact of water quality indicators on groundwater under multiple pollution sources. *Water*, *17*(6), 905.

Appendix 1. Overview of the DL Model Architectures

Model	Layer (Type)	Output Shape	Parameters
ANN	Dense	(None, 64)	1,344
	Dense	(None, 32)	2,080
	Dropout	(None, 32)	0
	Dense	(None, 16)	528
	Dense	(None, 1)	17
LSTM	LSTM	(None, 64)	1,088
	Dropout	(None, 64)	0
	Dense	(None, 32)	1,040
	Dropout	(None, 32)	0
	Dense	(None, 16)	544
	Dense	(None, 1)	33
Bi-LSTM	Bidirectional	(None, 64)	41,472
	Dropout	(None, 64)	0
	Dense	(None, 32)	18,560
	Dropout	(None, 32)	0
	Dense	(None, 16)	1,056
	Dense	(None, 1)	33

Supplementary Files

This is a list of supplementary files associated with this preprint. Click to download.

- Sheikhetal.2026Highlights.docx